LARAM School 2008 (7-22 September, Ravello, Italy)

SESSION 1: Landslide analysis using approaches based on: Geology, Geotechnics and Geomechanics

Basic Geodynamics of Landslides

II. The Dynamics of Landslide Run-out

Ioannis Vardoulakis

National Technical University of Athens

September 2008

http://geolab.mechan.ntua.gr/, I.Vardoulakis@mechan.ntua.gr

II. The Dynamics of Landslide Run-out

1. Rock falls: rolling vs. sliding 5
2. Run-out estimate 9
3. The sliding block on variable topography 11
4. Example 1: The frictionless circular track 15
5. Example 2: The frictional log-spiral track 17
6. Discussion 21
7. Limitations of the simple sliding block model 22
8. Appendix: Numerical integration of the governing non-linear o.d. eq.(5.1) 24
9. References 25

1. Rock falls: rolling vs. sliding

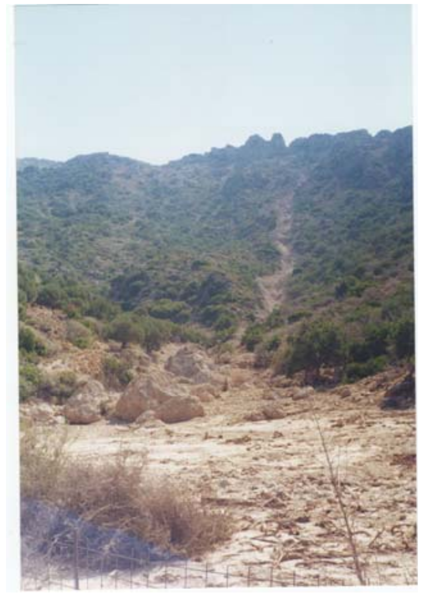

Figure 1-1: Rock fall triggered by heavy rain

A falling rock from high to low grounds will initially slide and roll (violent-fall phase) and finally it will only roll until it stops (tranquil-fall phase); Figure 1-1. In order to shed some light into these phenomena we consider here an idealized situation: A spherical object (the idealization of a large boulder) runs down a planar incline with a (constant) slope angle β (Figure 1-2.; cf. [11]).

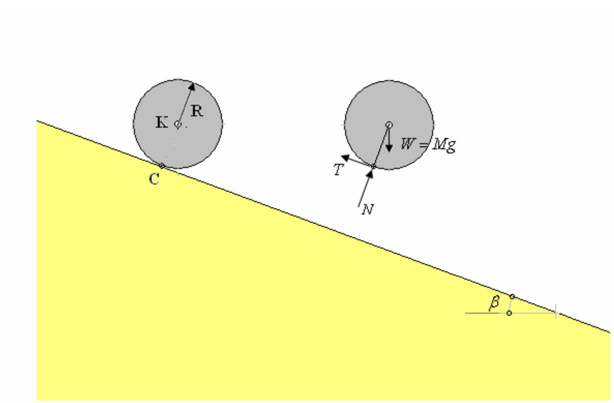

Figure 1-2: Sphere moving on a planar track

The motion of the sphere is described by the position $x_S(t)$ of its the center K and the rotation angle of the sphere $\varphi_S(t)$ with respect to an axis normal to plane of Figure 1-2 and passing through the center K of the sphere. Let M be the mass, R the radius and Θ_S the mass inertia of the sphere with respect to the aforementioned axis,

$$\Theta_S = \frac{2}{5}MR^2 \tag{1.1}$$

The forces that are acting on the sphere are the resultant force due to its self weight and the reaction forces at the point of contact. The weight,

$$W = Mg \tag{1.2}$$

is acting vertically on a line passing through the center K of the sphere. The reaction contact force is decomposed into a normal component N and a tangential component T.

The motion is assumed to be planar. Thus we will have three equations of motion; two for the translatory motion and one for the rotational motion. They derive from the corresponding balance equations for linear and angular momentum. In the considered case these equations are:

$$M\ddot{x}_S = Mg\sin\beta - T \tag{1.3}$$

$$0 = -Mg\cos\beta + N \quad \Rightarrow \quad N = Mg\cos\beta \tag{1.4}$$

$$\Theta_S\ddot{\varphi}_S = RT \tag{1.5}$$

We remark again that the equation in normal direction, eq. (1.4), is static because the track is considered to be planar.

If the sphere is rolling then its translation x_S must be equal to the arc from the new contact point to the old one (Figure 1-3),

$$x_S = R\varphi_S \tag{1.6}$$

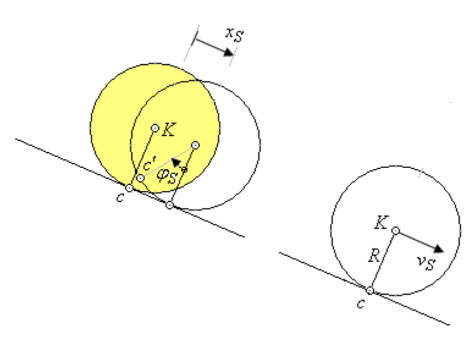

Figure 1-3: Rolling sphere on a planar track

Thus its translational and rotational velocities are kinematically constrained,

$$v_S = \dot{x}_S = R\dot{\varphi}_S \tag{1.7}$$

and also the accelerations,

$$a_S = \ddot{x}_S = R\ddot{\varphi}_S \tag{1.8}$$

From eqs. (1.5) and (1.3) we may eliminate the tangential force T and with eq. (1.8) we get an equation for the acceleration,

$$M\ddot{x}_S = Mg\sin\beta - \frac{\Theta_S}{R^2}\ddot{x}_S \tag{1.9}$$

or due to eq. (1.1),

$$\ddot{x}_S = \frac{5}{7}g\sin\beta \tag{1.10}$$

and form that and eq. (1.8),

$$\ddot{\varphi}_S = \frac{1}{R}\frac{5}{7}g\sin\beta \tag{1.11}$$

From eqs. (1.3) and (1.10) we get,

$$T = T_r = M\left(g\sin\beta - \ddot{x}_S\right) = \frac{2}{7}Mg\sin\beta \tag{1.12}$$

Let μ be the friction coefficient between sphere and the planar track. In order to exclude sliding we must assume that,

$$T \leq \mu N \tag{1.13}$$

or,

$$\mu \geq \frac{T_r}{N} = \frac{2}{7}\tan\beta \quad \Rightarrow \quad \mu < \tan\beta \leq \frac{7}{2}\mu \tag{1.14}$$

This means that in order to ensure rolling the tack inclination should not by too steep, i.e. if:

$$\mu < \tan\beta \leq 3.5\mu \Rightarrow rolling \tag{1.15}$$

Otherwise if

$$3.5\mu < \tan\beta \Rightarrow rolling + sliding \tag{1.16}$$

Ideally, rolling is a non-dissipative motion and the run-out distance for an ideally rolling sphere is infinite. This explains the fact that large boulders run-out large distances.

Ineq. (1.16), means that for very steep track inclinations ($\tan\beta > 3.5\mu$) we have to assume that the sphere rolls and slides simultaneously. In this case the tangential reaction is equal to the maximum frictional force,

$$T = \mu N \tag{1.17}$$

As the equations of motion clearly show, the tangential force as a frictional force decelerates the translational motion but it accelerates (due to its positive moment) the rotational motion,

$$\ddot{x}_S = g\cos\beta\left(\tan\beta - \mu\right) > 0 \tag{1.18}$$

$$\ddot{\varphi}_S = \frac{1}{R}\frac{5}{2}\mu g\cos\beta > 0 \tag{1.19}$$

Eq. (1.18) means that the fact that the object is rolling has no effect on its translational acceleration. The same acceleration would have the body even if it did not roll but it only slid along the track. The rotational acceleration is also the same as in the case of pure rolling, cf. eq. (1.11). Thus in the considered case of a steep track, the translational and the rotational motion, are not coupled to each other.

With decreasing track inclination, the translational acceleration drops gradually. As shown above, for values for $\tan\beta \leq 3.5\mu$ the sphere only rolls. Indeed, if we insert the value $\tan\beta = 3.5\mu$ into eq. (1.18) we get eq. (1.8). This means the transition from rolling and sliding to pure rolling is a smooth one.

2. Run-out estimate

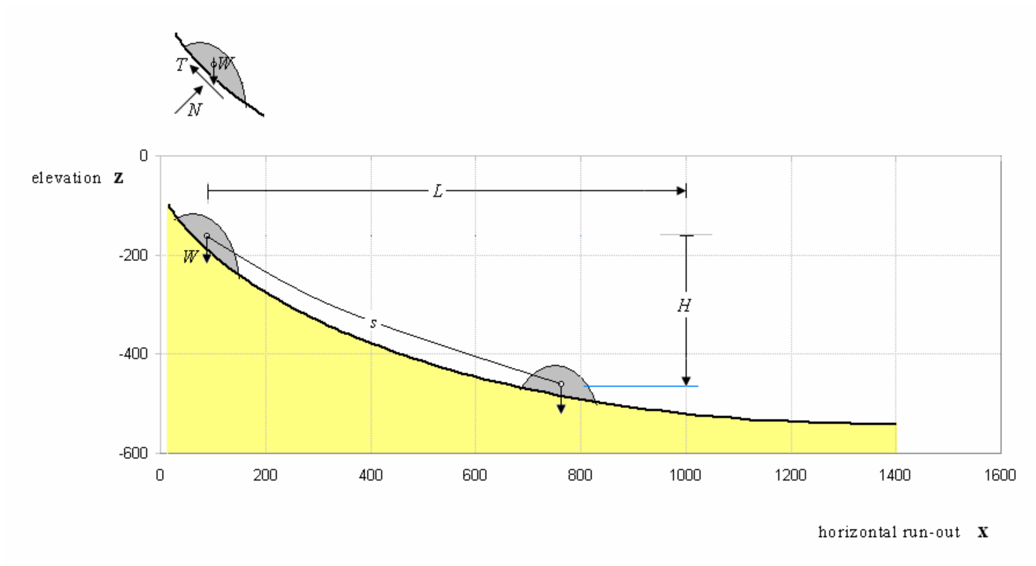

Figure 2-1: Run-out of rock-fall

An estimate of the run-out of a potential rockfall is computed as follows (cf. [2]; Figure 2-1): We consider the sliding rocks and earth masses lumped together as single object that is moving downslope. The total mass of this lump of moving earth-materials is M and its dead weight is

$$W = Mg \tag{2.1}$$

where g is the gravity acceleration. Mobilized by one of a number of possible trigger mechanisms this mass slides under the action of gravity with variable in time speed $V(t)$. Motivated by the ideal situation, discussed in the previous section, that rolling and sliding are uncoupled and that rolling is practically non-dissipative, all rolling of the rocks inside this lump is disregarded. This motion of the earth mass may be described by the energy balance equation that postulates the balance between changes in kinetic energy, the work done by the externally applied forces (i.e. the dead weight of the slide) and the energy dissipated due to the frictional contact of the earth mass along its track. Let dz be the change in elevation of the center of gravity of the debris and dD the energy dissipated for this increment of motion. Energy balance requires that the gain in kinetic energy equals to the work supplied by the dead weight during its fall (i.e. the loss in potential energy) minus the work dissipated due to sliding friction:

$$d\left(\frac{1}{2}MV^2\right) = Wdz - dD \tag{2.2}$$

Eq. (2.2) can be formally integrated along the path of the sliding mass. Let the length of this path be S and the corresponding fall height be H. At the origin and at the end of the sliding motion the velocity of the sliding mass is equal to zero; i.e. $V(0) = 0$ and $V(S) = 0$ Thus from eqs. (2.1) and (2.2) we get

$$M\int_0^S VdV = W\int_0^H dz - \int_0^S dD \quad \Rightarrow \quad 0 = WH - \int_0^S dD \tag{2.3}$$

The work dissipated during this motion is,

$$\int_0^S dD = \int_o^S Tds \tag{2.4}$$

where T is the friction force that is acted upon the sliding body by the track as a tangential to the track reaction contact force. Thus eq. (2.3) becomes,

$$\int_o^S Tds = WH \tag{2.5}$$

i.e. all the potential energy of the rock mass is dissipated by the shear force that develops at the base of it as frictional reaction. For purely frictional sliding, a simple Coulomb friction law may be assumed,

$$T = N\mu \tag{2.6}$$

where μ is a friction coefficient that is assumed here to be constant. Note that the introduction of μ implies no constraints on the details of the physics of rock fall run-out. In eq.(2.6) with N we denote the force that is acted upon the sliding body by the track as a normal to the track reaction contact force. In a first approximation we may set that,

$$N \approx W \cos\beta \tag{2.7}$$

The approximation refers to the neglect of centripetal accelerations (static equilibrium in normal direction; c.f. eq. (1.4)).Upon substitution of this closure for T and dD into eq. (2.5) we get,

$$WH = \mu W \int_o^S \cos\beta ds = \mu W \int_o^L dx = \mu WL \tag{2.8}$$

where L is the **horizontal** run-out. Thus

$$\frac{H}{L} = \mu \tag{2.9}$$

As we will se next this useful but simplified analysis disregards the effect of topography that in turn is reflected in a modification of eq. (2.7) that accounts for the effect of the centripetal force that develops when the slope inclination changes.

3. The sliding block on variable topography

The basic dynamics of landslide run-out can be introduced through a simple mechanical model. This model refers to a smooth and monotonously flattening topography of a sloping ground that is approximated here by a logarithmic spiral (Figure 3-1). The position of the sliding block on this track is given in polar coordinates by the position radius

$$R = a \exp(k\theta) \tag{3.1}$$

where, θ is the polar angle,

$$k = \cot\alpha \tag{3.2}$$

and α is the angle between the radius and the tangent to the log-spiral at the given position.

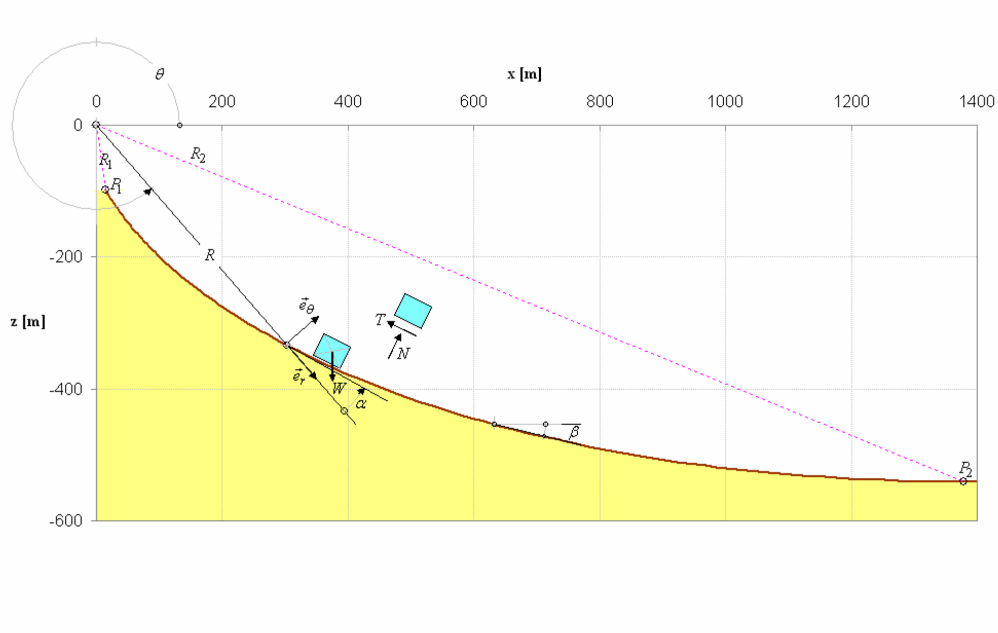

Figure 3-1: Smooth topography interpolated by a log-spiral, eq. (3.1)

For $\alpha = \pi/2$, we get that $k = 0$ and the track is a circular arc ($R = a = const.$). The slope angle at any point of the track is denoted by β and it relates to the other angular properties as,

$$\beta = 2\pi - (\alpha + \theta) \tag{3.3}$$

We notice that the traveled arc-length is,

$$s = \frac{\sqrt{1+k^2}}{k}(R - R_1) \tag{3.4}$$

The radius of curvature is linearly increasing with R,

$$R_c = R\sqrt{1+k^2} \tag{3.5}$$

For a circular arc $(k = 0)$, we get obviously that $R_c = R$.

Remark:

If we want to interpolate a given topography by such a curve we may choose two characteristic points, one uphill and another downhill, say the points $P_1(R_1, \theta_1)$ and

$P_2(R_2,\theta_2)$. From this input date we can compute the geometric parameters of the interpolating log-spiral, eq. (3.1), as,

$$\alpha = \arctan\left(\frac{\beta_1-\beta_2}{\ln\left(\frac{R_2}{R_1}\right)}\right) \quad ; \quad k = \cot\alpha \tag{3.6}$$

$$a = R_1 \exp\left(-k\theta_1\right) \tag{3.7}$$

We consider now the dynamic equations for a single block that slides down this track. The mass of the block is denoted again by M and its weight by W,

$$W = Mg \tag{3.8}$$

On that block are acting also the reaction force N and the friction force T, which at any instant are normal and parallel to the track, respectively. Let

$$\mu = \tan\varphi \tag{3.9}$$

be the Coulomb friction coefficient between the block and the track; φ is the corresponding Coulomb friction angle. While the block is in motion we set that

$$T = \mu N \tag{3.10}$$

The dynamic equations for the sliding block are written for the radial and circumferential components as follows

$$\begin{aligned} W_r + N_r + T_r &= Ma_r \\ W_\theta + N_\theta + T_\theta &= Ma_\theta \end{aligned} \tag{3.11}$$

In eqs. (3.11) with a_r and a_θ we denote the radial and tangential components of the block acceleration. Notice that in general the $r-$components are not normal to the track and the $\theta-$components are not tangential to the track. This is only the case for a circular track. The components of the acceleration in polar coordinates are,

$$a_r = \ddot{R} - R\dot{\theta}^2$$
$$a_\theta = R\ddot{\theta} + 2\dot{R}\dot{\theta} \tag{3.12}$$

where

$$R = R(t) \quad , \quad \dot{R} = \frac{dR}{dt} \quad etc \tag{3.13}$$

For the considered log-spiral, eq. (3.1), we get

$$a_r = R\left(k\ddot{\theta} + \left(k^2 - 1\right)\dot{\theta}^2\right)$$
$$a_\theta = R\left(\ddot{\theta} + 2k\dot{\theta}^2\right) \tag{3.14}$$

where

$$\theta = \theta(t) \quad , \quad \dot{\theta} = \frac{d\theta}{dt} \quad etc \tag{3.15}$$

The components of the forces acting on the block are,

$$W_r = -W\sin\theta \quad , \quad W_\theta = -W\cos\theta \tag{3.16}$$

$$N_r = -N\sin\alpha \quad , \quad N_\theta = N\cos\alpha \tag{3.17}$$

$$T_r = -\mu N\cos\alpha \quad , \quad T_\theta = -\mu N\sin\alpha \tag{3.18}$$

From eqs. (3.11) to (3.18) we get,

$$k\ddot{\theta} + \left(k^2 - 1\right)\dot{\theta}^2 = -\omega^2 e^{-k\theta}\left(\sin\theta + n\sin\left(\alpha + \varphi\right)\right)$$
$$\ddot{\theta} + 2k\dot{\theta}^2 = -\omega^2 e^{-k\theta}\left(\cos\theta - n\cos\left(\alpha + \varphi\right)\right) \tag{3.19}$$

where

$$\omega^2 = \frac{g}{a} \tag{3.20}$$

$$n = \frac{1}{\cos\varphi}\frac{N}{W} \tag{3.21}$$

The parameter ω introduces an inertial time-scale into the problem,

$$T = \omega^{-1} = \sqrt{\frac{a}{g}} \tag{3.22}$$

The parameter n is a dimensionless measure for the basal reaction forces. Notice that according to eqs.(3.10) and (3.21) we can express the reaction forces in terms of n,

$$\frac{N}{W} = n\cos\varphi \quad , \quad \frac{T}{W} = n\sin\varphi \tag{3.23}$$

4. Example 1: The frictionless circular track

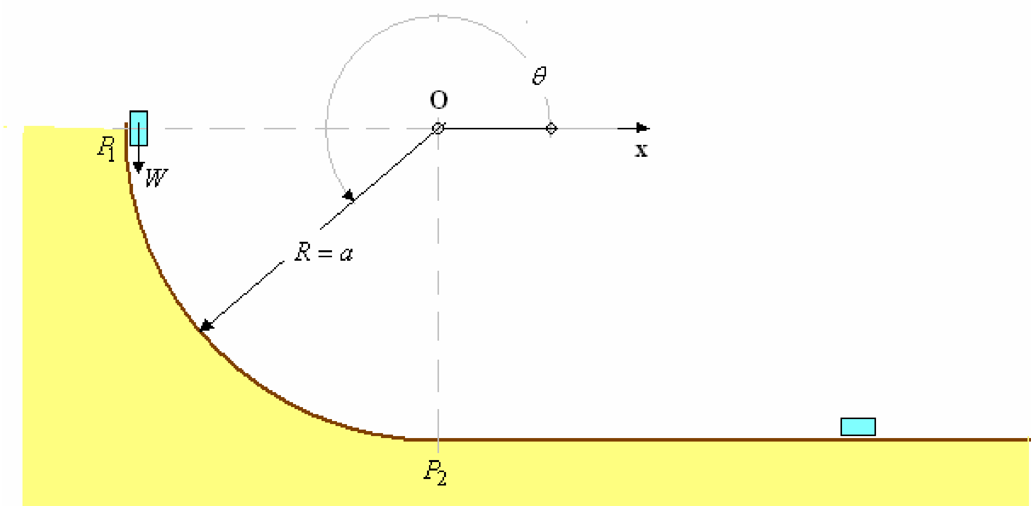

Figure 4-1: Circular track

We notice that for a circular tack ($R = a$, Figure 4-1) the dynamic eqs.(3.19) become,

$$k = 0 \quad \Rightarrow \begin{cases} \dot{\theta}^2 = \omega^2 \left(\sin\theta + n\cos\varphi \right) \\ \ddot{\theta} = -\omega^2 \left(\cos\theta + n\sin\varphi \right) \end{cases} \quad (4.1)$$

In particular for a <u>frictionless</u> circular tack we get an analytically integrable set of ordinary differential equations of motion,

$$\varphi = 0 \quad \Rightarrow \begin{cases} \dot{\theta}^2 = \omega^2 \left(\sin\theta + n \right) \\ \ddot{\theta} = -\omega^2 \cos\theta \end{cases} \qquad (4.2)$$

The second of eqs.(4.2) yields.

$$\ddot{\theta} = \frac{d\dot{\theta}}{d\theta}\frac{d\theta}{dt} = \dot{\theta}\frac{d\dot{\theta}}{d\theta} = -\omega^2 \cos\theta \quad \Rightarrow \quad \dot{\theta}d\dot{\theta} = -\omega^2 \cos\theta d\theta \qquad (4.3)$$

or

$$\frac{1}{2}\dot{\theta}^2 = -\omega^2 \sin\theta \qquad (4.4)$$

With this result we may compute the dimensionless normal force

$$n = \frac{N}{W} \qquad (4.5)$$

From the first of eq.(4.2) and eq. (4.4) we get

$$\omega^2 \left(\sin\theta + n \right) = 2\omega^2 \left(-\sin\theta \right) \quad \Rightarrow \quad n = 3\left(-\sin\theta \right) \qquad (4.6)$$

Eq. (4.6) means that the normal force is not constant but changes with the position.

From the first of eqs. (4.2) and eq. (4.6) we get further that,

$$\dot{\theta}^2 = 2\omega^2 \left(-\sin\theta \right) \qquad (4.7)$$

and with that the following expression for the circumferential velocity,

$$v_\theta = R\dot{\theta} = \sqrt{2ga\left(-\sin\theta \right)} \qquad (4.8)$$

Considering eq.(3.3) we get that the slope angle at any point of the circular track is

$$\beta = 3\pi / 2 - \theta \tag{4.9}$$

Thus

$$n = 3\cos\beta \tag{4.10}$$

The normal reaction amplification is due to the centripetal acceleration and assumes its maximum value at the lowest point of the track, where $\beta = 0$ and,

$$n_{\max} = 3 \tag{4.11}$$

This value is three times higher then the static value! Thus the transition from the curved track to a planar one is accompanied always with a sudden drop on the normal reaction force that is due to the sudden change in the curvature of the track.

The tangential velocity component

$$v_\theta = \sqrt{2ga\cos\beta} \tag{4.12}$$

assumes its maximum also at the lowest point of the circular track; i.e.

$$for \quad \beta = 0: \quad v_{foot} = v_{\theta,\max} = \sqrt{2ga} \tag{4.13}$$

5. Example 2: The frictional log-spiral track

In the case of a frictional, log-spiral track the resulting governing non-linear dynamic equations are,

$$A_0\ddot{\theta} + A_1\dot{\theta}^2 + A_2 e^{-k\theta}\sin\left(\theta + \alpha + \varphi\right) = 0 \tag{5.1}$$

where

$$\begin{aligned} A_1 &= k + \tan\left(\alpha + \varphi\right) \\ A_1 &= k^2 + 2k\tan\left(\alpha + \varphi\right) - 1 \\ A_2 &= \frac{\omega^2}{\cos\left(\alpha + \varphi\right)} \end{aligned} \tag{5.2}$$

and

$$n = -\frac{1}{\sin\left(\alpha+\varphi\right)}\left(\omega^{-2}e^{k\theta}\left(k\ddot{\theta}+\left(k^2-1\right)\dot{\theta}^2\right)+\sin\theta\right) \tag{5.3}$$

There is no analytic solution of eq. (5.1). Thus eq. (5.1) must be integrated numerically (cf. Sect. 8.). Using such a numerical integration scheme in Figure 5-1 we plotted the position of the sliding block as a function of time,

$$s = \frac{\sqrt{1+k^2}}{k}\left(R(t)-R_1\right) \quad , \quad R = a\exp\left(k\theta(t)\right) \tag{5.4}$$

In Figure 5-2 we plotted the velocity of the sliding block along this track,

$$v_t = v_r \cos\alpha + v_\theta \sin\alpha \tag{5.5}$$

where

$$v_r = kR\dot{\theta} \quad , \quad v_\theta = R\dot{\theta} \tag{5.6}$$

As can be seen from Figure 5-2 the maximum velocity does not correspond to the lowest position, as this was the case in the frictionless circular track.

For low friction angles the sliding block continues its journey on the flat terrain for some distance until its velocity becomes zero. So, if v_{foot} is the velocity of the block at the foot of the track ($\beta = 0^\circ$), then the run-out distance on the flat is,

$$s_{flat} = \frac{3}{2}\frac{v_{foot}^2}{\mu g} \tag{5.7}$$

In Figure 5-3 we plotted the sliding block acceleration as function of time,

$$a_t = a_r \cos\alpha + a_\theta \sin\alpha \tag{5.8}$$

where

$$a_r = kR\ddot{\theta} + (k^2-1)R\dot{\theta}^2 \quad , \quad a_\theta = R\ddot{\theta} + 2kR\dot{\theta}^2 \tag{5.9}$$

We observe that initially the block is accelerating and later on, it decelerates as it enters a region of small sloping angles with respect to the assumed basal friction. When the block enters the flat a small acceleration jerk is taking place, that is related to the discontinuous change in the basal normal reaction (curvature change). In Figure

5-4 we plotted the normal reaction force that is excreted onto the sliding block at various times. We observe that in this example the maximum dynamic value is about 20% higher then the static value. In the same figure we observe the aforementioned discontinuous change in the basal normal reaction that is due the non-smooth transition from the curved track to the planer track; cf. eq. (3.5)

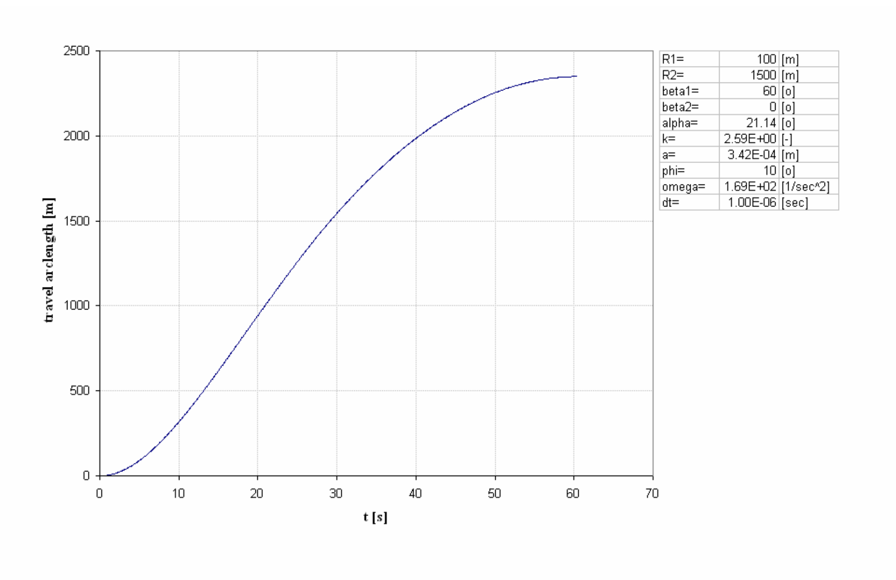

Figure 5-1: Position of the sliding block as function of time

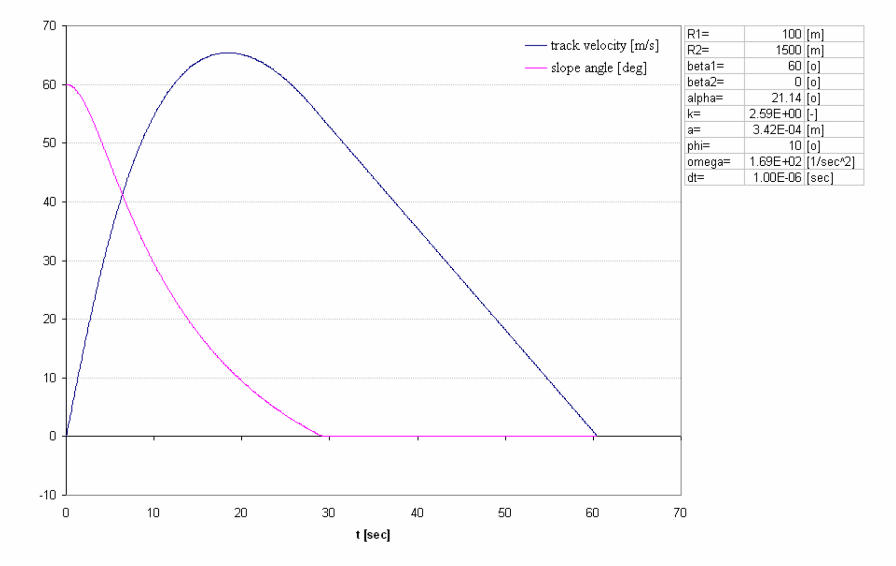

Figure 5-2: Sliding block velocity as function of time. The magenta curve indicates the slope at any time the block is experiencing along the variable topography

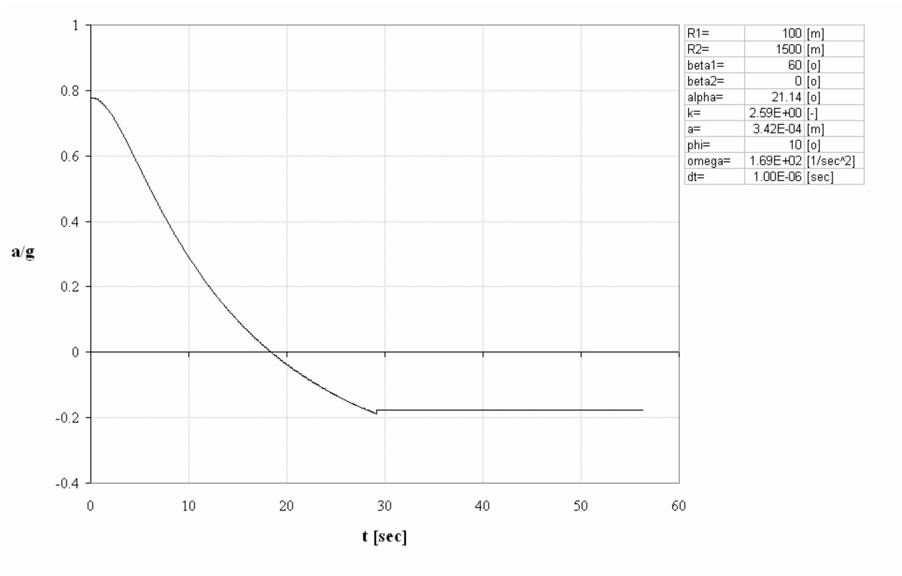

Figure 5-3: Sliding block acceleration as function of time

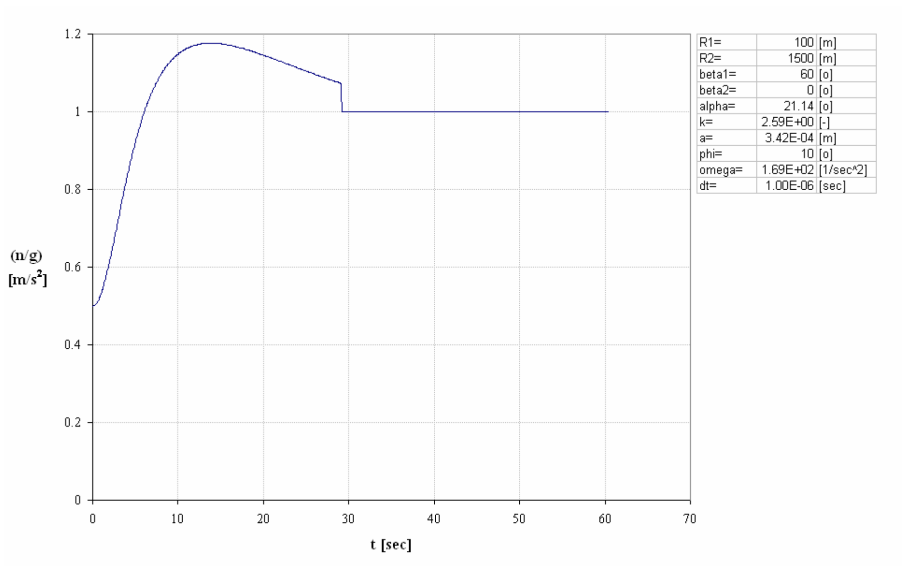

Figure 5-4: Normalized normal reaction force as function of time

6. Discussion

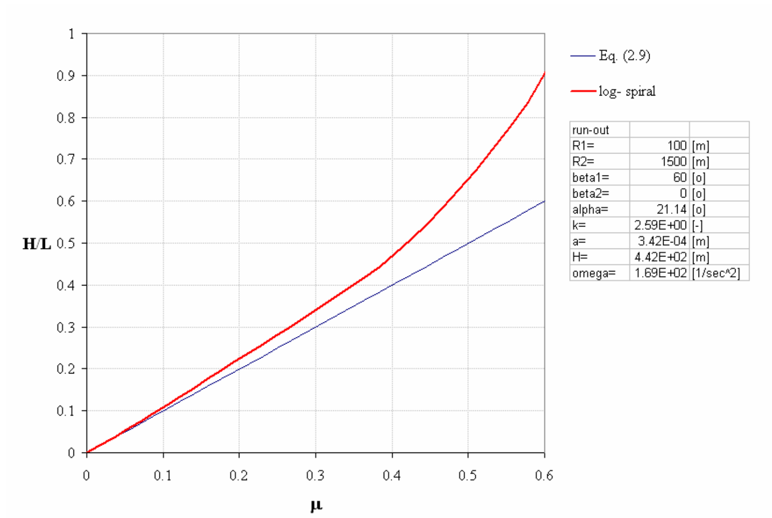

Figure 6-1: Run-out ratio as a function of the friction coefficient for a log-spiral track

As can be seen from Figure 6-1, for low basal friction values,

$$\frac{H}{L} \approx \mu \tag{5.10}$$

is a rather good estimate for the sliding block run-out distance. However for large values of the basal friction the effect of the topographically amplified normal reaction force is felt and the run-out distance is turning out to be rather small (i.e. the ratio H/L increases more than linearly).

As was first noticed by Heim [12], catastrophic landslides are characterized by a very large (L/H)-value, thus indicating the appearance of a very small friction coefficient. Indeed field data suggest a reduction of the friction coefficient, $\mu \approx (H/L)$, with the volume of the landslide (Figure 6-2). This observation has triggered intensive research efforts for the disclosure of possible mechanisms that would explain this severe reduction in frictional resistance. Recent studies on catastrophic landslides corroborate the original "vaporization" concept of Habib [9],[10]. The idea that a heat generating mechanism might account for the total loss of strength of large earth slides due to thermal pressurization of the pore fluid inside the failure zone has been discussed in the past by Uriel & Molina [19] , Goguel [8], Anderson [1], Voight & Faust [18], and more recently by Vardoulakis [15],[16], Garagash & Rudnicki [5], Goren & Aharonov [7] and de Blasio [4].

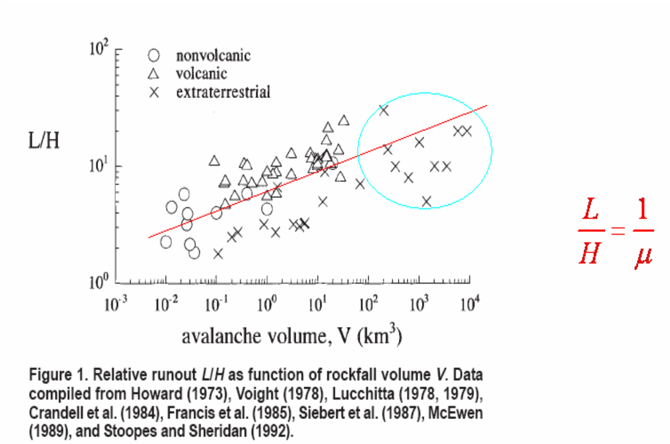

Figure 6-2: Taken from Dade & Huppert [2]

7. Limitations of the simple sliding block model

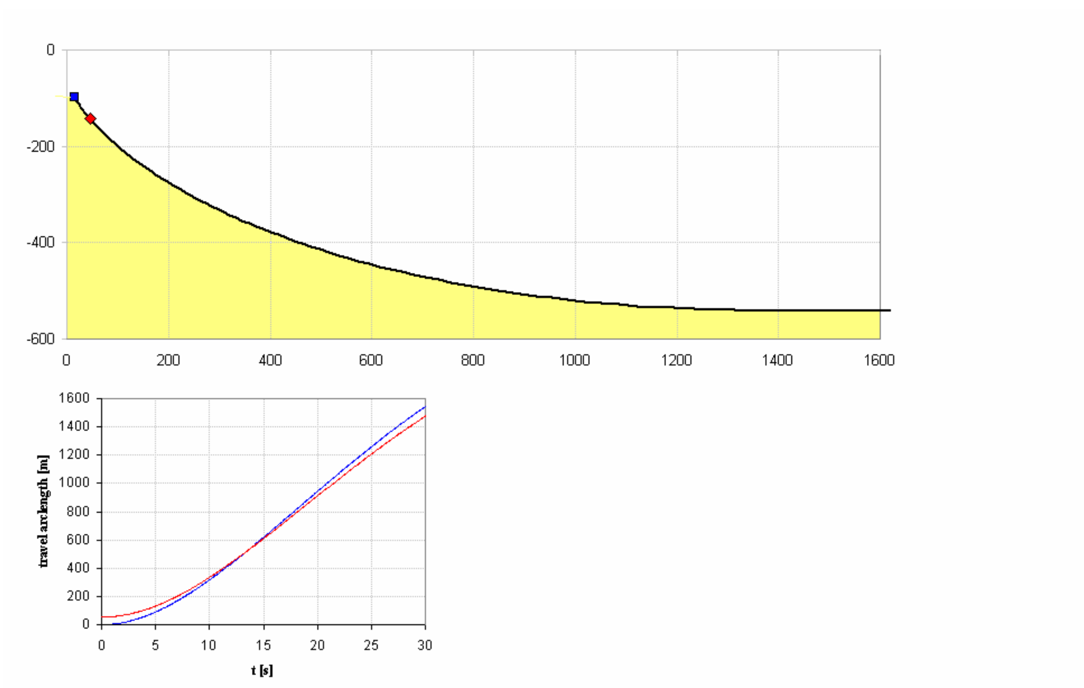

Figure 7-1: The travel lines of two neighboring blocks

As can be seen in Figure 7-1, if we consider two neighboring blocks (blue and red in figure) and we release them simultaneously, then they will soon collide, since the upper block will try to overtake the lower one. This means that the single block model is of relatively limited value. In reality the various rock masses which exist at various elevations will interact with lateral earth-pressure forces, which in turn will decelerate slightly the upper blocks and accelerate slightly the lower blocks, so that a common acceleration is established for the whole mass. This consideration leads inevitably to the so-called flow-slides models, which are derived from shallow-water type theories (Savage & Hutter [14]).

8. Appendix: Numerical integration of the governing non-linear o.d. eq.(5.1)

Here the *"method of curvature"* (Davis [3]) is applied. According to this method the integration is done as follows: Let,

$$\ddot{\theta} = f\left(t, \theta, \dot{\theta}\right) \tag{8.1}$$

with the initial values at time $t_0 = 0$,

$$\begin{aligned} \theta(0) &= \theta_0 \\ \dot{\theta}(0) &= \dot{\theta}_0 \end{aligned} \tag{8.2}$$

Then from (8.1) and (8.2) we get,

$$\ddot{\theta}(0) = f\left(t_0, \theta_0, \dot{\theta}_0\right) \tag{8.3}$$

Then at time $t_1 = t_0 + \Delta t$ the method of curvature yields,

$$\begin{aligned} \theta_1 &= \theta_0 + \dot{\theta}_0 \Delta t + \frac{1}{2} \ddot{\theta}_0 \Delta t^2 \\ \dot{\theta}_1 &= -\frac{\ddot{\theta}_0 \Delta t + \dot{\theta}_0 \left(1 + \dot{\theta}_0^2\right)}{\ddot{\theta}_0 \left(\dot{\theta}_0 \Delta t + \frac{1}{2} \ddot{\theta}_0 \Delta t^2\right) - \left(1 + \dot{\theta}_0^2\right)} \\ \ddot{\theta}_1 &= f\left(t_1, \theta_1, \dot{\theta}_1\right) \end{aligned} \tag{8.4}$$

The error is estimated as

$$\varepsilon = \frac{3}{2} \frac{\dot{\theta}_i \ddot{\theta}_i^2}{1 + \dot{\theta}_i^2} \Delta t^2 \tag{8.5}$$

The algorithm is recursive.

Here we used the following initial values,

$$\begin{aligned} \theta_0 &= given \\ \dot{\theta}_0 &= 0 \end{aligned} \tag{8.6}$$

9. References

[1] Anderson, D.L. (1980). An earthquake induced heat mechanism to explain the loss of strength of large rock and earth slides. Int. Conf. on Engineering for Protection from natural disasters, Bangkok.

[2] Dade, W. B. and H. E. Huppert (1998), Long-runout rockfalls, Geology, 26(9), 803– 806.

[3] Davis, H.T., Introduction to Nonlinear Differential and Integral Equations, Dover, 1962.

[4] De Blasio, F.V. (2008). Production of frictional heat and hot vapour in a model of self-lubricating landslides. Rock Mechanics and Rock Engineering, 41, 219-226.

[5] Garagash, D.I. and Rudnicki, J.W. (2003). Shear heating of a fluid-saturated slip-weakening dilatant fault zone: 1. Limiting regimes. Journal of Geophysical Research, 108 (B2), 2121, doi: 1029/2001JB001653.

[6] Goguel, J. (1978). Scale-dependent rockslide mechanisms, with emphasis on the role of pore fluid vaporization. Ch. 20, pp. 693-705, in: "Developments in Geotechnical Engineering, Vol. 14a, Rockslides and Avalances, 1, Natural Phenomena. Barry Voight, ed., Elsevier.

[7] Goren, L. and Aharonov, E. (2007). Long runout landslides: The role of frictional heating and hydraulic diffusivity. Geophysical Research Letters, 34 (7): Art. No. L07301

[8] Goguel, J. (1978). Scale-dependent rockslide mechanisms, with emphasis on the role of pore fluid vaporization. Ch. 20, pp. 693-705, in: "Developments in Geotechnical Engineering, Vol. 14a, Rockslides and Avalances, 1, Natural Phenomena. Barry Voight, ed., Elsevier.

[9] Habib, P. (1967). Sur un mode de glissement des massifs rocheaux. C. R. Hebd. Seanc. Acad. Sci., Paris, 264, 151-153.

[10] Habib, P. (1975). Production of gaseous pore pressure during rock slides. Rock Mech., 7, 193-197.

[11] Hauger., W, Schnell, W. und Gross, D., *Technische Mechanik, Bd. 3:Kinetik*, Springer Verlag, 1989.

[12] Heim, A.. *Bergsturtz und Menschenleben*. Fretz u. Wasmuth, Zürich, 1932.

[13] Romero, S.U. and Molina, R. (1974). Kinematic aspects of the Vaiont slide. Proc. 3rd Congress Int. Soc. Rock Mechanics, Denver, Vol. II, Part B, 865-870.

[14] Savage, S.B. and Hutter, K. (1989). The motion of a finite mass of granular mate-rial down a rough incline. J. Fluid Mech. 199, 177-215.

[15] Vardoulakis, I. (2000). Catastrophic landslides due to frictional heating of the failure plane. Mech. Coh. Frict. Mat., 5, 443-467

[16] Vardoulakis, I. (2002). Dynamic thermo-poro-mechanical Analysis of Catastrophic Landslides. Géotechnique, 52,No.3,157-171.

[17] Veveakis, E., Vardoulakis, I. and Di Toro G.(2007). Thermo-poro-mechanics of creeping landslides: the 1963 Vaiont slide, Northern Italy. Journal of Geoephysical Research, accepted for publication.

[18] Voight, B. and C. Faust (1982). Frictional heat and strength loss in some rapid landslides. Géotechnique, 32, 43-54.

[19] Uriel, R.S. and Molina, R. (1974). Kinematic aspects of the Vaiont slide. Proc. 3rd Congress Int. Soc. Rock Mechanics, Denver, Vol. II, Part B, 865-870.